2013 IEEE International Conference on Control Applications (CCA)
Part of 2013 IEEE Multi-Conference on Systems and Control
Hyderabad, India, August 28-30, 2013

Sliding mode control of a buck converter for maximum power point tracking of a solar panel

Amir Hussain, Avanish Kumar, Laxmidhar Behera
Department of Electrical Engineering,
Indian Institute of Technology Kanpur
Email: amirh@iitk.ac.in, avanishk@iitk.ac.in, lbehera@iitk.ac.in

***Abstract*—This paper presents a novel sliding mode control (SMC) approach for maximum power point tracking (MPPT) of photovoltaic (PV) panel using buck converter. Since classical hill climbing and incremental conductance MPPT methods can not differentiate change in power due to perturbed voltage and changing weather condition, both algorithms are prone to failure in case of rapidly varying solar radiation. Most of the maximum power point tracking approaches presented in literature are based on finding desired PV voltage for MPPT and tracking the actual PV voltage to desired one. On contrary, in this paper, SMC approach is applied to control inductor current and converter output voltage for MPPT and then convergence and tracking of PV voltage is achieved. Incremental conductance method is used to find desired value of PV voltage and steady state analysis is performed on state equation to find out desired inductor current and output voltage of converter. The proposed controller is able to bring the system on sliding surface in finite time and force it to remain on sliding surface. It has been found that exact MPPT is achieved even when we consider varying atmospheric condition and disturbances. The feature of the proposed algorithm are supported by theoretical analysis and simulation results.**

***Index Term*—photovoltaic system, DC-DC converters, sliding mode control, steady state error, MPPT.**

I. INTRODUCTION

Photovoltaic system is the technology that uses solar cells or an array of them to convert solar light directly into electricity. The power produced by the array depends on cells temperature and solar irradiation. Usually the energy generated by these solar cells is used to provide electricity to a load and the remaining energy is saved into batteries. A major challenge in the use of PV is posed by its nonlinear currentvoltage (IV) characteristics, which result in a unique maximum power point (MPP) on its powervoltage (PV) curve. The challenge becomes more difficult because panel voltage and current corresponding to MPP keeps changing with variation in cell temperature and solar radiation.

Several methods have been designed and implemented to search for this operation point among which common tracking schemes are perturb and observe (P&O) [1]-[3], incremental conductance [4]-[7], short circuit current [8], open circuit voltage [9]. Some modified techniques have also been proposed, with the objective of minimizing the hardware or improving the performance [10]-[13]. In P&O method, the panel voltage is constantly perturbed by varying duty cycle of converter in order to achieve MPPT. In incremental conductance method, change in terminal voltage and array current are measured to predict the effect of change of voltage on power output. The above MPPT algorithms can be realized with guaranteed convergence stability. However, both of the methods need large step of perturbation for fast convergence which results in more chattering around MPPT. Also, the change in output power does not purely reflect the effect of change in perturbed voltage because power may be changed by changing weather condition too.

In this paper, we propose SMC to regulate duty cycle of dc-dc buck converter in order to force the PV module to operate at its maximum power point. In a typical sliding mode control [12] approach, the first objective is to choose a proper sliding surface (SS) such that if system state is on sliding surface, it is driven to zero. The designed controller must bound the system to remain on SS. Second objective is choose a controller which force the system to reach SS. The sliding mode controller has robust control property under the presence of parameter variations and can achieve the tight regulation of the states for all operating points [15].

II. SYSTEM MODELING

A. PV characteristic

A PV cell can be represented by current source with diode and two resistances connected as shown in Fig.1. Where R_s is relatively small and R_p is relatively large, which are neglected in the equation in order to simplify the simulation.The mathematical expression of the equivalent model can be written as (1)-(3).

$$I_o = I_g - I_s(e^{(\beta v_o)} - 1) \tag{1}$$

$$I_g = (I_{sc} + k_I(T - Tr))\lambda/\lambda_r \tag{2}$$

$$I_s = I_r \left(\frac{T}{T_r}\right)^3 e^{qE_{gp}(\frac{1}{T_r} - \frac{1}{T})/pK} \tag{3}$$

where, I_o is output current from single PV cell, I_g is light generated current, I_d the current through diode which is replaced by diode equation and I_s the reverse saturation current of diode, I_r is the reverse saturation current at the reference temperature T_r (298 K), E_{gp} = 1.1 eV is the

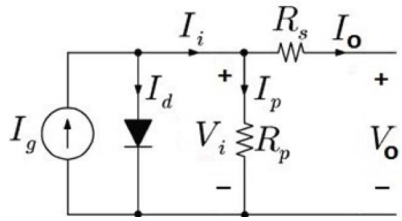

Fig. 1. Single diode model of PV cell.

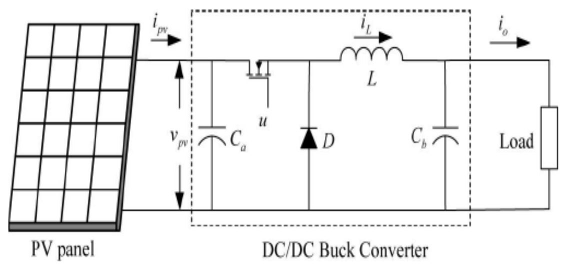

Fig. 2. PV array in conjunction with a buck converter.

bandgap energy of the semiconductor used in the cell, I_{sc} is the short-circuit cell current at reference temperature and solar irradiation, k_I (in milliamperes per kelvin) is the short-circuit current temperature coefficient, λ is the irradiance (in milliwatts per square centimeter) and λ_r is reference radiation level (100 mW/cm2). β is inverse thermal voltage given by,

$$\beta = \frac{q}{pKT}$$

where, q = 1.6 x 1019 C is charge of an electron, K = 1.3805 x 1023 J/K is Boltzmanns constant, T cell temperature, and p is ideality factor. Now if PV module is made up of n_s cells connected in series and n_p cells connected in parallel then output current of PV module is given by,

$$i_{pv} = n_p I_g - n_p I_s (e^{(\beta v_{pv}/n_s)} - 1) \tag{4}$$

B. Power Converter

Fig. 2 shows a PV array connected to a dc-dc buck converter. Power output from PV module is controlled by varying the duty cycle of buck converter so as to operate at a voltage at which Power output can be maximized. The state space model of buck converter can be given by the following equation,

$$\dot{\mathbf{x}} = \mathbf{f(x)} + \mathbf{g(x)}u \tag{5}$$

$$\mathbf{x} = [x_1, x_2, x_3]'$$

$$\mathbf{f(x)} = [f_1(x), f_2(x), f_3(x)]'$$

$$\mathbf{g(x)} = [g_1(x), g_2(x), g_3(x)]'$$

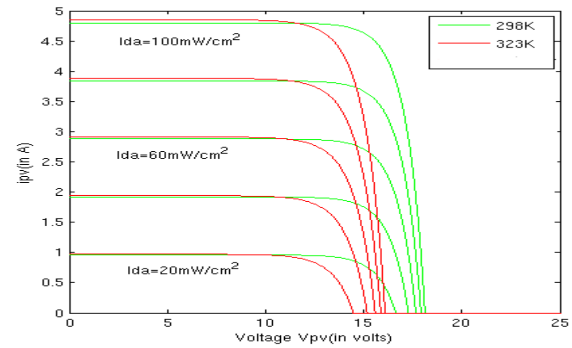

Fig. 3. IV characteristic of solar panel at different cell temperature and solar radiation.

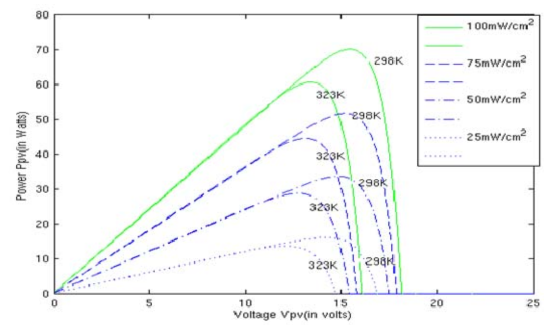

Fig. 4. PV characteristic of solar panel at different cell temperature and solar radiation.

$$f_1(x) = \frac{1}{L}\left[\left(\frac{R_b}{R_{ld}} - 1\right)x_3 - (R_b + R_l)x_1 - V_d\right]$$

$$f_2(x) = \frac{1}{C_a}\left[n_p I_g - n_p I_s (e^{(\beta x_2/n_s)} - 1)\right]$$

$$f_3(x) = \frac{1}{C_b}\left(x_1 - \frac{x_3}{R_{ld}}\right)$$

$$g_1(x) = \frac{(V_d + x_2)}{L}$$

$$g_2(x) = -\frac{x_1}{C_a}$$

$$g_3(x) = 0 \tag{6}$$

where

x_1 = Inductor current(A)
x_2 = Panel voltage(V)
x_3 = Output voltage(V)
I_{pv} = Current drawn from solar panel(A)
u = Duty cycle
C_a = Input capacitor(F)
C_b = Output capacitor(F)

III. DESIGN OF SLIDING MODE CONTROLLER

While applying sliding mode control, the most important concern is selection of sliding surface. There may exist infinite number of sliding surfaces for a system but all of them do not brings the system to origin. Furthermore, if sliding surface comprises lesser number of states than the order of system, the controller must stabilize all those states which are not included in sliding surface. A sliding surface is presented in [15] which comprises error in PV voltage and inductor current as sliding states considering i_{pv} as a constant. For smaller change in solar radiation i_{pv} may be assumed constant but for large change in irradiance, i_{pv} must be considered as variable for choosing sliding surface and controller design. Considering above constraints, a sliding surface is chosen taking error in inductor current and converter output voltage as sliding states. The chosen surface needs desired value of inductor current and converter output voltage which are calculated in the sequel.

A. *Calculation of desired states*

Incremental conductance method with an added inner loop is used to calculate desired value of PV voltage. Calculation is made fast by taking larger step size in inner loop when error is more and step size is decreased gradually when it reaches sufficiently close to the desired value. Since, calculation of desired value does not involve controller (which is fixed between 0 to 1), the system is always stable and calculation is made fast without any significant chattering. Hence application of incremental conductance method for calculating desired value is free from the demerits of chattering or slow convergence in case of rapid change in weather condition. Calculation of desired value of inductor current and converter output voltage is performed as follows

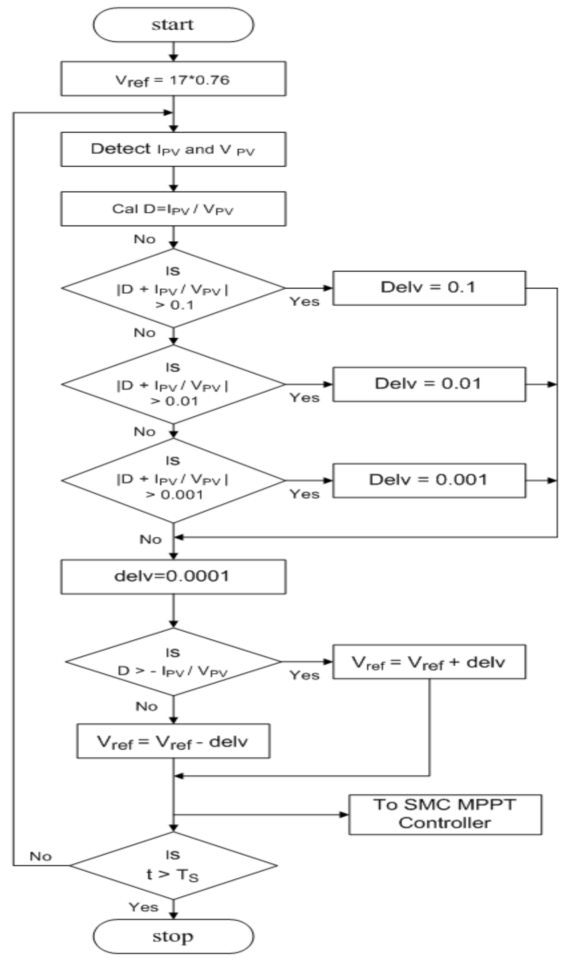

Fig. 5. Flow chart for calculation of desired panel voltage.

In desired condition

$$e_1 = e_2 = e_3 = 0, \dot{e}_1 = \dot{e}_2 = \dot{e}_3 = 0$$

Assuming x_{1r}, x_{2r}, x_{3r} to be desired value of inductor current, PV voltage and converter output voltage respectively and using above equation for inductor current,

$$\frac{1}{L}[(\frac{R_b}{R_{ld}} - 1)x_3 - (R_b + R_{ld})x_1 - V_D] + \frac{(V_D + x_2)}{L}u = \dot{x}_{1r}$$

$$(V_D + x_{2r})u = L\dot{x}_{1r} + V_D + (R_b + R_{ld})x_{1r} - (\frac{R_b}{R_{ld}} - 1)x_{3r} \tag{7}$$

similarly for converter output voltage, following equation can be derived

$$\dot{x}_{1r}u = n_pI_g - n_pI_s(e^{\frac{\beta x_{2r}}{n_s}} - 1) - C_a\dot{x}_{2r} \tag{8}$$

Dividing (8) by (9) to eliminate u

$$\frac{V_D + x_{2r}}{x_{1r}} = \frac{L\dot{x}_{1r} + V_D + (R_b + R_{ld})x_{1r} - (\frac{R_b}{R_{ld}} - 1)x_{3r}}{n_pI_g - n_pI_s(e^{\frac{\beta x_{2r}}{n_s}} - 1) - C_a\dot{x}_{2r}} \tag{9}$$

Now we have eliminate x_1 and its derivative in order to get direct relation between x_{2r} and x_{3r} and their derivatives. using steady state for capacitor output voltage,

$$x_{1r} = \frac{x_{3r}}{R_{ld}} + C_b\dot{x}_{3r} \tag{10}$$

and

$$\dot{x}_{1r} = \frac{\dot{x}_{3r}}{R_{ld}} + C_b\ddot{x}_{3r} \tag{11}$$

substituting (10) and (11) in equation (9)

$$\ddot{x}_{3r} = (A/B - C)\frac{1}{LC_b} \tag{12}$$

where

$$A = (V_D + x_{2r})(n_pI_g - n_pI_s(e^{\frac{\beta x_{2r}}{n_s}} - 1) - C_a\dot{x}_{2r})$$

$$B = C_b\dot{x}_{3r} + \frac{x_{3r}}{R_{ld}}$$

$$C = \frac{L\dot{x}_{3r}}{R_{ld}} + (R_b + R_{ld})B + V_D - (\frac{R_b}{R_{ld}} - 1)x_{3r}$$

Once $\ddot{x}_{3r}$ is known, x_{3r} and $\dot{x}_{3r}$ can be updated. Also, using (11) x_{1r} will be updated.

B. Choosing sliding surface

Rewriting dynamic equation for converter output voltage as

$$\dot{x}_3 = \frac{1}{Cb}(x_1 - \frac{x_3}{R_{ld}}) \tag{13}$$

when desired condition is reached, $\dot{x}_3 = \dot{x}_{3r}$

$$\dot{x}_{3r} = \frac{1}{Cb}(x_{1r} - \frac{x_{3r}}{R_{ld}}) \tag{14}$$

Using above two equations, the error dynamics can be found as

$$\dot{e}_3 = \frac{1}{Cb}(e_1 - \frac{e_3}{R_{ld}}) \tag{15}$$

now choosing sliding surface as

$$s = e_1 + ke_3 \tag{16}$$

when system is on sliding surface,

$$s = 0 \Rightarrow e_1 = -ke_3$$

putting value of e_1 in (15)

$$\dot{e}_3 = -\frac{1}{Cb}(k + \frac{1}{R_{ld}})e_3 \tag{17}$$

similarly, using sliding condition and (15) the dynamics of e_1 can be written as

$$\dot{e}_1 = -\frac{1}{Cb}(k + \frac{1}{R_{ld}})e_1 \tag{18}$$

Above two equations show that e_1 and e_3 converges to zero if

$$\frac{1}{Cb}(k + \frac{1}{R_{ld}}) > 0 \tag{19}$$

Choosing $k > 0$ above condition is easily satisfied and time taken for e_1 and e_3 to converge to a small value ε is

$$t_\varepsilon = \frac{C_b}{K + \frac{1}{R_{ld}}} ln \left[\frac{|e(0)|}{|\varepsilon|}\right]$$

where, t_ε is time taken for e_1 and e_3 to converge to small value ε and e_0 is initial value of e_1 and e_3. It can be observe from (17) and (18) that time constant for converge for e_1 and e_3 is same. Therefore, both error converges together if system is on sliding surface. Also, C_b is in order of μF, time constant is very low even for smaller value of k.

C. Sliding mode Controller

When system is on sliding surface, the equivalent control input is obtained by substituting $\dot{s} = 0$

$$\dot{e_1} + k\dot{e_3} = 0$$

$$\dot{x}_1 - \dot{x}_{1r} + k(\dot{x}_3 - \dot{x}_{3r}) = 0$$

$$f_1(x) + g_1(x)\hat{u} - \dot{x}_{1r} + k(f_3(x) - \dot{x}_{3r}) = 0$$

$$\hat{u} = \frac{-f_1(x) + \dot{x}_{1r} - k(f_3(x) - \dot{x}_{3r})}{g_1(x)}$$

Above controller bounds the system on sliding surface once it is reached on sliding surface. If system is not on sliding surface, above controller can not be applied. To bring system on sliding surface, controller can be modified as

$$u = \hat{u} - \frac{k_1 \mathrm{sgn}(s)}{g_1(x)} \tag{20}$$

Controller in (20) brings the system on sliding surface with a constant rate which makes convergence very slow. To make it fast, (20) can again be modified as

$$u = \hat{u} - \frac{k_1 \mathrm{sgn}(s) + k_2 s}{g_1(x)} \tag{21}$$

D. Convergence and tracking of PV voltage

Writing state equation for PV voltage as

$$\dot{x_2} = \frac{1}{C_a}(n_p I_g + n_p I_s - x_1 u) - \frac{n_p I_s}{C_a}(e^{(\beta x_2/n_s)}$$

$$\dot{x_2} = k_3 - k_4(e^{(\beta x_2/n_s)} \tag{22}$$

where, k_3 is bounded quantity and k_4 is a positive constant. Above equation can be proved for x_2 to be bounded if both k_3 and k_4 are strictly positive. Noting that u is between 0 to 1 and inductor current is always less than the generated current in PV system, k_3 is always positive. Hence x_2 is also bounded and stability of whole system is guaranteed with SMC. Now, performing steady state analysis for tracking of x_2 to its desired value. In steady state

$$\dot{x_3} = \frac{1}{C_b}\left(x_1 - \frac{x_3}{R_{ld}}\right) = 0$$

Therefore x_1 and x_3 are bounded by

$$x_3 = x_1 R_{ld} \tag{23}$$

Similarly, performing steady state analysis on inductor current and capacitor output voltage results in,

$$(V_d + x_2)n_p I_g + n_p I_s - n_p I_s e^{\frac{\beta x_2}{n_s}} + (R_{ld} + R_l)x_1^2 + V_D x_1 = 0 \tag{24}$$

Above relation represent a quadratic equation in x_1 which has one positive and one negative solution for a particular value of x_2. Since inductor current can not flow in opposite direction in converter, negative solution of x_1 is not possible. Hence, there is only one possible solution for x_1 exists for one value of x_2 in steady state. Also, from (23), x_3 has only one solution for a particular x_1. Hence all the three states of PV system are bounded by one to one mapping in steady state.

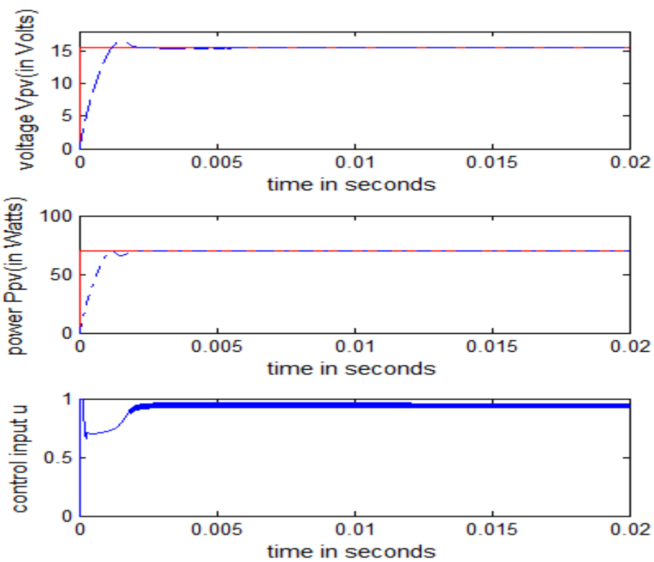

Fig. 6. MPPT control response at $298K$ and $100mW/cm^2$ (a)Red line: MPP voltage, blue dash: obtained voltage by SMC,(b) Red line :Power at MPP Blue dash: obtained power by SMC and (c) control input u(t).

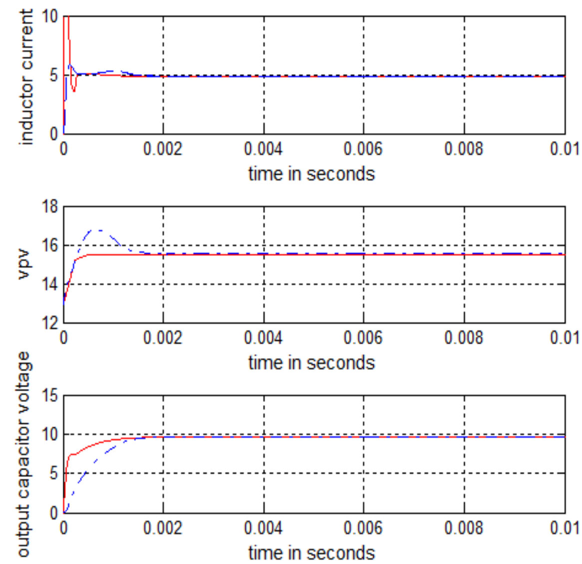

Fig. 7. MPPT control response at $298K$ and $100mW/cm^2$ (a) Red line: Desired , Blue dash: obtained inductor current (b) Red line:Desired, Blue dash: obtained PV array voltage and (c) Red line: Desired , Blue dash: obtained output capacitor voltage.

In PV system, for a particular cell temperature and solar radiation, there exists only one desired value of panel voltage for MPPT. Since all the states are bounded by one to one relation, there exists only one value of desired inductor current and converter output voltage for a particular weather condition. Therefore, if inductor current and converter output voltage are converging to their desired value, PV voltage must reach to its desired value provided system remains stable during the course of convergence.

IV. Simulation Results

The simulation of this solar power system has been carried out to verify the theoretical results. The specifications of the Solar Panel are as follows: Number of cells in parallel, $n_p = 1$ and the number of cells in series, $n_s = 36$. Short circuit current, $I_{sc} = 4.8A$. Short circuit current temperature coefficient, $k_I = 2.06mA/^0C$. The specifications of the Dc-Dc converter are as follows: Storage Inductance (L) of $95\mu H$, Capacitance's $C_a = 200\mu F$ and $C_a = 300\mu F$. The internal resistances R_b and R_l of capacitance C_b and Inductance L are chosen as $162m\Omega$ and 1Ω respectively. The forward voltage drop of the power diode D, v_D is taken as 0.7 Volts. Incremental value of each step is calculated from the flow chart. Frequency of searching algorithm is set at $10KHz$. Fig.6-8 shows simulation of the above solar panel using SMC when we consider fixed temperature and solar radiation at $298K$ and $100mW/cm^2$ respectively. The controller gains are chosen as $k_1 = 3000$ and $k_2 = 300$. These high values of k_1 and k_2 is justified as value of $g_1(x)$ is 2 order higher than controller gains. Fig. 6. shows that MPPT voltage and extracted power from PV array reach their desired values with in 3-4 ms. In Fig. 8. convergence of errors of system states in shown. It has been found that all errors converges to zero asymptotically and with in 2-3 ms and they are found to be

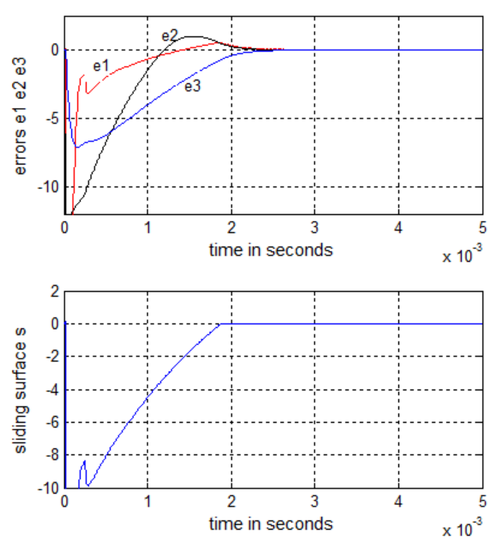

Fig. 8. MPPT control response at $298K$ and $100mW/cm^2$(a) error in inductor current e_1, error in PV array voltage e_2 and error in output capacitor voltage e_3 (b) waveform of sliding surface.

sufficiently close to zero. Next, we have simulated our system under varying temperature and solar radiation as shown in Fig. 9. Tracking of output capacitor voltage, output power and control input are depicted in Fig. 10. Error in inductor current, panel voltage and output capacitor voltage are shown in Fig. 11 under varying cell temperature and solar radiation.

V. Conclusion

In this paper, MPPT control strategy based on sliding mode theory has been presented for PV solar power generation

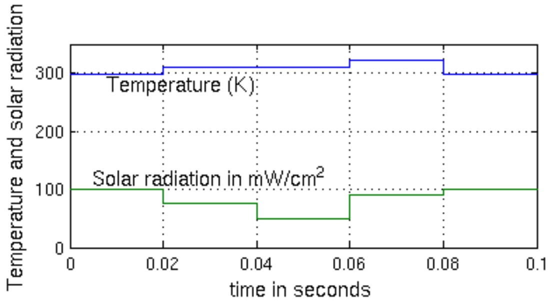

Fig. 9. variation in temperature and solar radiation.

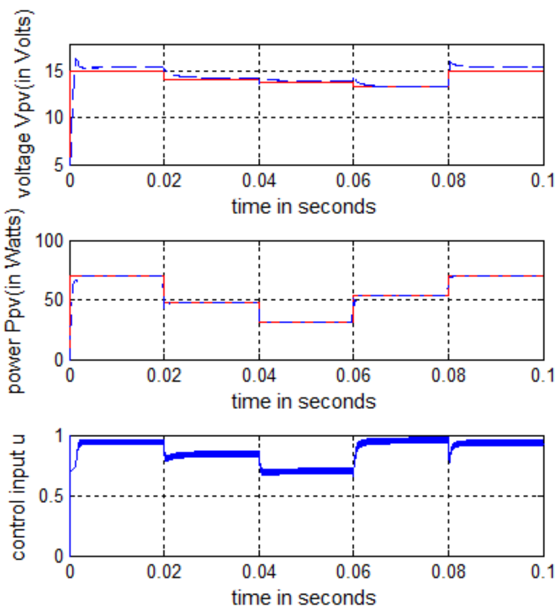

Fig. 10. MPPT control response under varying temperature and solar radiation ((a) Red line: MPP voltage, blue dash : obtained voltage by SMC,(b) Red line :Power at MPP Blue dash : obtained power by SMC and (c) control input u(t).

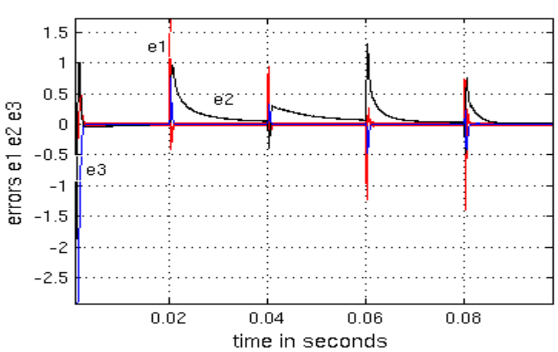

Fig. 11. Error in inductor current e_1, error in PV array voltage e_2 and error in output capacitor voltage e_3.

system . A dc-dc buck converter is used to control the voltage so as to ensure MPPT. Error dynamics has been derived for the system and from that a sliding surface is chosen to ensure the convergence of all system states to desired values. The control diagram proposed is very simple, using a global model of the nonlinear system, and from which a nonlinear control law directly applied to the power switch. In the presence of the disturbance and uncertainty, the robust MPPT is also assured while the maximum power tracking error is attenuated to a prescribed level. Compared with the traditional PI controller, proposed SMC achieves fast tracking response with precise control and significantly less chattering. Thus, proposed SMC control assures better tracking performance with high robustness.

REFERENCES

[1] Z. Salameh and D. Taylor, "Step-up maximum power point tracker for photovoltaic arrays", *Solar Energy,* vol. 44, no. 1, pp. 57-61, 1990.

[2] G. Carannante, C. Fraddanno, M. Pagano, and L. Piegari," Experimental performance of MPPT algorithm for photovoltaic sources subject to inhomogeneous insolation," *IEEE Trans. Ind. Electron.,* vol. 56, no. 11, pp. 4374-4380, Nov. 2009.

[3] H. Patel and V. Agarwal, "MPPT scheme for a PV-fed single-phase singlestage grid-connected inverter operating in CCM with only one current sensor," *IEEE Trans. Energy Convers.,* vol. 24, no. 1, pp. 256-263, Mar. 2009.

[4] K. H. Hussein, I. Muta, T. Hoshino, and M. Osakada, "Maximum photovoltaic power tracking: An algorithm for rapidly changing atmospheric condition," *Proc. Inst. Electr. Eng., Gen. Transmiss. Distrib.,* vol. 142, no. 1, pp. 59-64, 1995.

[5] K. H. Hussein and I. Muta, "Maximum photovoltaic power tracking: An algorithm for rapidly changing atmospheric conditions", *Proc. Inst. Electr. Eng.Generation, Transmission Distribution,* vol. 142, no. 1, pp. 59-64, Jan. 1995.

[6] T. Noguchi, S. Togashi, and R. Nakamoto, "Short-current pulse-based maximum-power-point tracking method for multiple photovoltaic and converter module system," *IEEE Trans. Ind. Electron.,* vol. 49, no. 1, pp. 217-223, Feb. 2002.

[7] C. Dorofte, U. Borup, and F. Blaabjerg, "A combined two-method MPPT control scheme for grid-connected photovoltaic systems," *in Proc. Eur. Conf. Power Electron. Appl.,* Sep. 1114, 2005, pp. 1-10.

[8] D. Sera, T. Kerekes, R. Teodorescu, and F. Blaabjerg, "Improved MPPT method for rapidly changing environmental conditions," in *Proc. IEEE Int. Ind. Electron. Symp.,* Jul. 2006, vol. 2, pp. 1420-1425.

[9] N. Kasa, T. Iida, and H. Iwamoto, "Maximum power point tracking with capacitor identifier for photovoltaic power system," *Proc. Inst. Electr. Eng.Electr. Power Appl.,* vol. 147, no. 6, pp. 497-502, Nov. 2000.

[10] N. Kasa, T. Iida, and L. Chen, "Flyback inverter controlled by sensorless current MPPT for photovoltaic power system," *IEEE Trans. Ind. Electron.,* vol. 52, no. 4, pp. 1145-1152, Aug. 2005.

[11] M. Veerachary, T. Senjyu, and K. Uezato, "Maximum power point tracking control of IDB converter supplied PV system," *Proc. Inst. Electr. Eng.Electr. Power Appl.,* vol. 148, no. 6, pp. 494-502, Nov. 2001.

[12] J.J.E.Slotine and W.Li. *Applied Nonlinear Control.* Prentice hall, New Jersey, 1991.

[13] Stanishlaw H. Zak. *System and Control.* Oxford University Press, New York, 2003.

[14] Chian-Song Chiu,Ya-Lun Ouyang, Chan-Yu Ku, "Terminal sliding mode control for maximum power point tracking of photovoltaic power generation systems", *Solar Eneargy.,* Vol. 86, no. 10, pp. 2986-2995, Oct. 2012.

[15] Domingo, Biel, Enric, Fossas, et al., 2001. "Application of sliding-mode control to the design of a buck-based sinusoidal generator", *IEEE Trans. Ind. Electron.* Vol. 48, no. 3, pp. 563-571, Jun. 2001.